

On the Photo-Disintegration of the Deuteron by Lithium and Fluorine γ -Rays

P. V. C. HOUGH*

Laboratory of Nuclear Studies, Cornell University, Ithaca, New York

(Received July 7, 1950)

The photographic emulsion has been used to measure the differential cross section for the photo-disintegration of the deuteron by 6.1- and 7.0-Mev γ -rays, and by 14.8- and 17.6-Mev γ -rays. A new method for the absolute measurement of γ -ray intensities leads to an absolute value for the total cross section at 17.6 Mev of $(7.2 \pm 1.5) \times 10^{-28}$ cm². The results are in agreement with the theory for a "free" deuteron *P*-wave, but are not sufficiently accurate to fix with greater precision any of the parameters in the neutron-proton potential.

I. INTRODUCTION

IT was first pointed out by Powell¹ in 1940 that the photographic plate allows a new measurement of the cross section for the photo-disintegration of the deuteron. Since the war Gibson, Green, and Livesey,² and Goldhaber³ have exploited the technique, using deuteron-loaded emulsions. They employed for their source the 6.1-Mev and 7.0-Mev gamma-radiation which results from the bombardment of fluorine by protons. The present paper (Section II) reports an extension of their work which yields an angular distribution of the photo-disintegration protons at the mean energy of the fluorine γ -rays.

The use of deuteron-loaded emulsions for recording disintegrations by higher energy γ -rays is complicated by the onset of competing (γ, p) processes in other elements in the emulsion. Fast neutrons, produced by (γ, n) reactions in surrounding material, also contribute to the background through collision with emulsion protons and deuterons. As described in Section III, both background components have been eliminated, and differential and absolute total cross-section measurements have been made from the 14.8- and 17.6-Mev γ -rays obtained by the bombardment of lithium with protons. The absolute cross-section measurement depends on a new method for the absolute measurement of γ -ray intensities which was suggested by R. R. Wilson and is described in Section IV.

While these experiments were in progress, Waffler and Younis⁴ reported an absolute measurement of the total cross section for the photo-disintegration by lithium γ -rays. Also, Fuller⁵ published preliminary results for the differential cross section at various γ -ray energies as well as a measurement of the relative total cross section as a function of energy, using the bremsstrahlung beam from a 22-Mev betatron. Since then Goldhaber⁶ has reported measurements of the differential cross section using fluorine γ -rays, and Barnes,

Stafford, and Wilkinson,⁷ total cross sections for γ -rays from both fluorine and lithium. The measurements of these experimenters are compared with the present results, and the experiments compared with the theory, in Section V.

II. DISINTEGRATION BY FLUORINE γ -RAYS

As was first demonstrated by Goldhaber,³ nuclear emulsions can absorb large amounts of heavy water and still record low energy proton tracks. In the present investigation two Kodak NTB 100-micron plates were loaded with 34 mg/cm² of D₂O and 33 mg/cm² of H₂O respectively. The plates were then irradiated with γ -rays produced by the bombardment of a thick sodium fluoride target with 1.1-Mev protons from the Cornell cyclotron. Vapor-tight aluminum cassettes supported the plates, with their emulsions in the plane of the cyclotron target plate. With the geometrical arrangement in this plane shown in Fig. 1, an exposure from 100 μ amp-hrs. of protons was found to be satisfactory. The plates were processed by standard techniques, except that the usual pre-soak in water was already accomplished during the exposure.

For observation, the emulsion area was divided by light scratches into squares about 2 mm on a side. The provision of small, definite search areas which can be examined in a single observation period has many advantages. It allows different observers to work conveniently on a single plate. It allows the plate to be removed and replaced without introducing uncertainty in the coordinates. Most important of all, it permits unambiguous comparison of the accuracies of different observers.

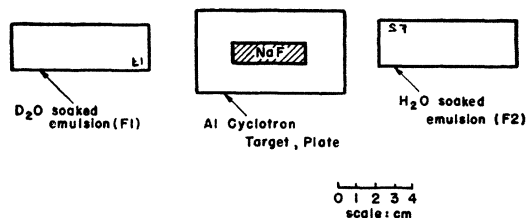


FIG. 1. Arrangement of the photographic emulsions with respect to the sodium fluoride target for the exposure to the fluorine γ -rays.

⁷ Barnes, Stafford, and Wilkinson, *Nature* **165**, 70 (1950).

* Now at the University of Michigan, Ann Arbor, Michigan.

¹ C. F. Powell, *Nature* **145**, 155 (1940).

² Gibson, Green, and Livesey, *Nature* **160**, 534 (1947).

³ G. Goldhaber, *Phys. Rev.* **74**, 1725 (1948).

⁴ H. Waffler and S. Younis, *Helv. Phys. Acta* **22**, 414 (1949).

⁵ E. G. Fuller, *Phys. Rev.* **76**, 576 (1949); **77**, 647 (1950); **79**, 303 (1950).

⁶ G. Goldhaber, *Phys. Rev.* **77**, 753 (1950).

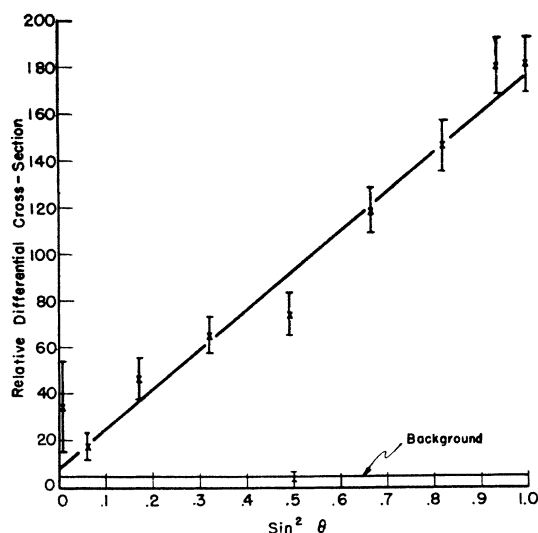


FIG. 2. Relative differential cross section at the mean energy of the fluorine γ -rays.

The search of a 1.3-cm² area of the D₂O-loaded emulsion yielded 1034 tracks beginning and ending in the emulsion, or an area density of about 800 tracks/cm². The H₂O-loaded emulsion showed an area density of similar tracks which was 4 percent of this number.

In determination of the angular distribution of the photo-protons, tracks of very great dip angle are rejected because of the unknown and probably smaller efficiency for their detection. (The dip angle of a track is the complement of the angle the track makes with the normal to the emulsion surface. The polar angle, θ , and azimuthal angle, α , used here and in Section IV, refer to a spherical coordinate system, with the polar axis parallel to the emulsion surface and in the direction of propagation of the gamma-radiation.) If δ_0 is the maximum dip angle considered, tracks of polar angle $\delta_0 < \theta < \pi - \delta_0$ are selected only if they lie in a range of azimuthal angle compatible with the restricted dip angle. Furthermore, for the larger values of $\sin\theta$, a few tracks are lost because they pierce the emulsion surface. This loss is small (always less than 5 percent) because the average track length is only about one-sixth of the wet emulsion thickness.

A simultaneous consideration of both of these effects shows that the fraction $f(\theta)$ of tracks recorded at polar angle θ is

$$f(\theta) = 1 - (\lambda/\pi) \sin\theta, \quad \theta < \delta_0$$

$$= (2/\pi) \arcsin(\sin\delta_0/\sin\theta) - (\lambda/\pi) [\sin\theta - (\sin^2\theta - \sin^2\delta_0)^{1/2}], \quad \theta > \delta_0, \quad (1)$$

where λ = mean track length (65μ) \div wet emulsion thickness (385μ) = 0.17, and δ_0 is the cut-off dip angle.

The searching and track measurement were carried out by three observers, with concordant results. All tracks observed were recorded and selections made afterward to form a group of dip less than $4\mu/35\mu$, and another of dip less than $6\mu/35\mu$. The reduction of

measured dip angles to true unprocessed wet-emulsion dip angles requires a knowledge of the emulsion thickness under the conditions of the exposure. Micrometer measurements on other plates of the same emulsion number established that water and emulsion volumes add to within 5 percent. Thus, the measured weight of D₂O added to the emulsion gives for its thickness during the exposure $385 \pm 20\mu$. The true maximum dip angles for the two groups of tracks considered are 56° and 67° .

The detection efficiency of the observers was found by the Rutherford method of coincidence observing to be only about 70 percent. This low efficiency is a consequence of the wet emulsion exposure, which gave weak tracks. However, possible forward or 90° observer bias was removed by the survey of half the total emulsion area with the plate at right angles to its usual position. Also, no evidence was found for any systematic variation in detection efficiency with dip angle (up to the maximum values accepted).

As a check, the length of each track was recorded. The distribution in range obtained showed a strong peak at 65μ and a smaller peak, not completely resolved, at about 90μ . The corresponding energies deduced for the fluorine γ -ray lines are 6.2 and 7.0 Mev, in agreement, within experimental error, with the more accurate measurements of Walker and McDaniel.⁸

The results of the angular distribution measurement are shown in Table I. The second column gives the number of tracks of dip angle less than 67° and with polar θ relative to the γ -ray in the range shown in column 1. (The group with $\delta_0 = 56^\circ$ was found to give an angular distribution in agreement within statistics, but is not shown because it is not statistically independent and is of less statistical weight.) Column 3 is column 2 divided by $f(\theta)$ and thus gives the total numbers of tracks which occur in the various ranges of θ . Column 4 is column 3 divided by $(10/2\pi)$ times the solid angle available for the photo-protons in each angular range and hence is proportional to the differential cross section for the photo-disintegration. Throughout, tracks at angle $\pi - \theta$ are grouped with those at angle θ , because in most cases it was impossible to determine the direction of motion of the proton. Figure 2

TABLE I. The angular distribution of photo-protons at the mean energy of the fluorine γ -rays.

Polar angle θ°	Observed number of tracks $\delta_0 = 67^\circ$	Corrected number of tracks	Relative differential cross section
0-9	4	4	34 ± 20
10-19	7	7	17 ± 6
20-29	30	30	46 ± 9
30-39	56	58	65 ± 8
40-49	79	82	74 ± 9
50-59	144	151	119 ± 10
60-69	194	209	147 ± 11
70-79	208	275	181 ± 12
80-90	227	321	182 ± 12

⁸ R. L. Walker and B. D. McDaniel, Phys. Rev. **74**, 315 (1948).

shows the relative differential cross section plotted against $\sin^2\theta$. The background, measured on the H_2O -loaded plate and assumed to be isotropic, is also indicated. The straight line through the data points was determined by least squares. If we write the differential cross section in the form,

$$\sigma(\theta) = \sigma_t(a + \sin^2\theta) / 4\pi(a + \frac{2}{3}), \quad (2)$$

where σ_t is the total cross section, the least squares line gives

$$a = 0.02 \begin{matrix} +0.04 \\ -0.02 \end{matrix}$$

The lower limit of error is determined by the fact that a is non-negative, and the upper limit is the r.m.s. deviation from the mean.⁹

The ratio, τ , of the photo-magnetic to photoelectric total cross section is simply $(3a/2)$,¹⁰ provided the contribution of the tensor force to the isotropic component in the differential cross section is negligible.¹¹ On this assumption we have at the mean fluorine γ -ray energy of 6.4 Mev,

$$\tau = 0.03 \begin{matrix} +0.06 \\ -0.03 \end{matrix} \quad (3)$$

The theoretical value¹⁰ for τ at this energy is 0.02, neglecting P -state forces entirely.

III. DISINTEGRATION BY LITHIUM γ -RAYS

The well-known lithium γ -rays, of energies 14.8 and 17.6 Mev, were obtained by the bombardment of a thick lithium metal target with 0.75-Mev protons from the Cornell cyclotron. D_2O - and H_2O -loaded emulsions were exposed to this radiation, as in the work described

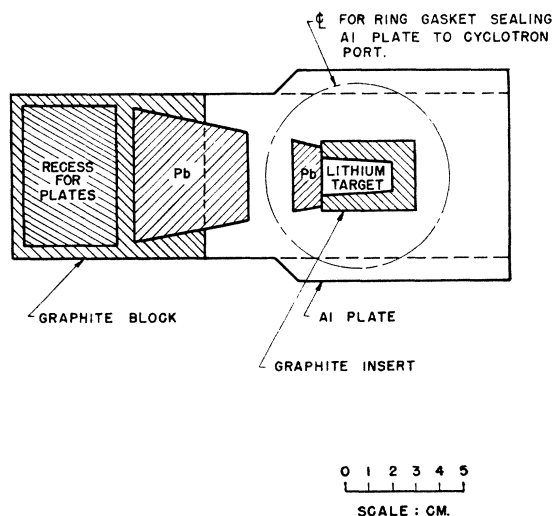


FIG. 3. Combination cyclotron target plate and plate holder for the exposure to the lithium γ -rays.

⁹ Whittaker and Robinson, *The Calculus of Observations* (Blackie and Son, London, 1924), Chapter IX.

¹⁰ H. A. Bethe, *Elementary Nuclear Theory* (Wiley, 1947).

¹¹ W. Rarita and J. Schwinger, *Phys. Rev.* **59**, 436, 556 (1941).

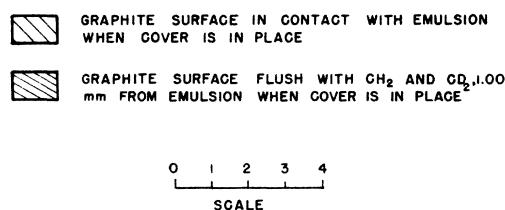
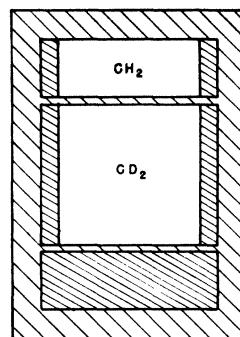


FIG. 4. Graphite cover for the plate holder shown in Fig. 3.

above. Now, however, preliminary measurements showed no significantly larger number of tracks in the D_2O -loaded emulsion.

It was decided, therefore, to shield the emulsion from the direct gamma-radiation and to study the disintegrations occurring in a thin slab of deuterated paraffin (CD_2), placed parallel to the emulsion and a few millimeters away in the full γ -ray beam. In this way (γ, p) processes occurring in the emulsion are suppressed, while photo-protons from the CD_2 can cross the short air space to the emulsion to be recorded. A minimum emulsion range of 53μ was required for acceptance of a track for measurement, and this criterion excludes all tracks from the reaction $\text{C}^{12}(\gamma, p)\text{B}^{11}$. The plate holder itself was made of graphite, so that the possibility of a background due to (γ, p) reactions is eliminated.

The possibility remains, however, that some tracks entering the emulsion from the CD_2 slab are fast deuterons resulting from the impact of photo neutrons. To investigate this point, a section of the CD_2 "radiator" was replaced with CH_2 . Since the (n, p) scattering cross section is slightly larger than the (n, d) cross section over the relevant neutron energy range, the number of tracks from the CH_2 gives a (close) upper bound to the number of recoil deuterons. It was found in this way that in an early arrangement about 20 percent of the tracks originating in the CD_2 were actually deuteron recoils. The photo-neutron flux was then reduced by introducing a graphite insert into the cyclotron aluminum target plate where the γ -ray intensity is high, by decreasing the thickness perpendicular to the γ -ray beam of the lead sheet which shields the emulsion, and by surrounding the plate holder with a several-foot thick paraffin shield. The recoil deuteron

TABLE II. Area density of tracks in various regions of the emulsion after exposure to lithium γ -rays.

Region	Tracks/cm ²
Opposite CD ₂	17.0±1.0
Opposite CH ₂	2.6±0.6
Opposite graphite	2.7±0.7
Unexposed plate	3.3±1.5

component was eliminated by these measures, although which were essential is not known.

The combination cassette and cyclotron target plate is shown in Fig. 3 with the cassette cover removed. The top surfaces of the lead shield and the lithium target are in one plane, with the emulsion surface parallel to this plane and 0.50±0.05 mm below. The CH₂ and CD₂ are melted into recesses in the cassette cover (Fig. 4), so that their free surfaces are in a plane parallel to and 1.00±0.05 mm from the emulsion surface when the cover is in place. Thus the CD₂ nearest the emulsion surface is 0.50±0.08 mm above the surface of the lead and definitely unshielded by lead. There is 6.4 cm of paraffin, 1.2 cm of graphite, and 1.2 cm of rubber between the source and the CD₂ during the exposure. One region of the emulsion surface faces simply graphite, and it is this part which is scanned to verify that (γ , p) reactions in the emulsion are really eliminated. The completeness of the background eradication may be judged from the track area densities given in Table II.

As in the work with fluorine γ -rays, the detection sensitivity of the arrangement is not independent of the angle of motion of the proton and must be calculated. To formulate the problem precisely, we choose rectangular coordinates in the surface of the CD₂ radiator with the x -axis in the direction of the gamma-radiation. The thickness of the radiator is greater than the maximum range of the disintegration protons. If θ is the polar angle relative to the x -axis and α is the azimuth angle, the number of recorded tracks in solid angle $\sin\theta d\theta d\alpha$ coming from the radiator area element $dx dy$ is

$$d^4n = \epsilon G(x) \sigma(\theta) \sin\theta d\theta d\alpha \cdot Nz(\theta, \alpha) dx dy, \quad (4)$$

where ϵ is the detection efficiency of the observer, $G(x)$ is the total number of γ -rays/cm² at position (x, y) (to sufficiently good approximation G is independent of y), $\sigma(\theta)$ is the differential cross section for the photo-disintegration, and N is the number of deuterons per cm³ of heavy paraffin. $z(\theta, \alpha)$ denotes the total thickness of paraffin in which a proton can originate and cause a track at angles θ, α , whose projected length in the emulsion is at least 53 μ and which stops before entering the glass. (The first criterion is designed to assure a high observer efficiency, and the second to eliminate from consideration the many cosmic-ray tracks which traverse the emulsion completely.) Since momentum and energy conservation determines the energy of a disintegration proton, and therefore also its range in paraffin and in the emulsion, it is a matter of geometry

to determine $z(\theta, \alpha)$. The integration of (4) over α and over x and y is elementary, and without giving further details we write the result as follows:

$$dn = \epsilon \Gamma t N A Z(\theta) \sigma(\theta) \sin\theta d\theta / 4\pi x_1 x_2. \quad (5)$$

Here dn represents the observed number of tracks in the range $d\theta$ at θ , Γ is the total number of γ -rays emitted by the source during the exposure, t represents the transmission of the material between the source and the radiator (0.85), x_1 is the distance from the center of the source to the nearest edge of the CD₂ radiator (13.6 cm), x_2 is the distance to the farthest edge (17.4 cm), and A is the area of the radiator (14.5 cm²). Evidently $Z(\theta)$ can be interpreted as the average thickness of the radiator times the average range of azimuth angle for which disintegration protons at polar angle θ are recorded.

Actually, for the two lithium γ -rays, we must replace $Z\sigma$ in Eq. (5) by $Z_1\sigma_1[I_1/(I_1+I_2)] + Z_2\sigma_2[I_2/(I_1+I_2)]$, where I_1, I_2 are the intensities of the low and high energy lines respectively. If we define

$$\bar{Z} = Z_1[\sigma_1 I_1 / (\sigma_1 I_1 + \sigma_2 I_2)] + Z_2[\sigma_2 I_2 / (\sigma_1 I_1 + \sigma_2 I_2)], \quad (6)$$

$$\bar{\sigma} = \sigma_1 [I_1 / (I_1 + I_2)] + \sigma_2 [I_2 / (I_1 + I_2)],$$

this replacement gives simply

$$dn = \epsilon \Gamma t N A \bar{Z}(\theta) \bar{\sigma}(\theta) \sin\theta d\theta / 4\pi x_1 x_2. \quad (7)$$

Using the measured intensity ratio¹² $I_1/I_2=0.52$ and the Bethe-Peierls theoretical ratio¹⁰ $(\sigma_1/\sigma_2)=1.24$, one

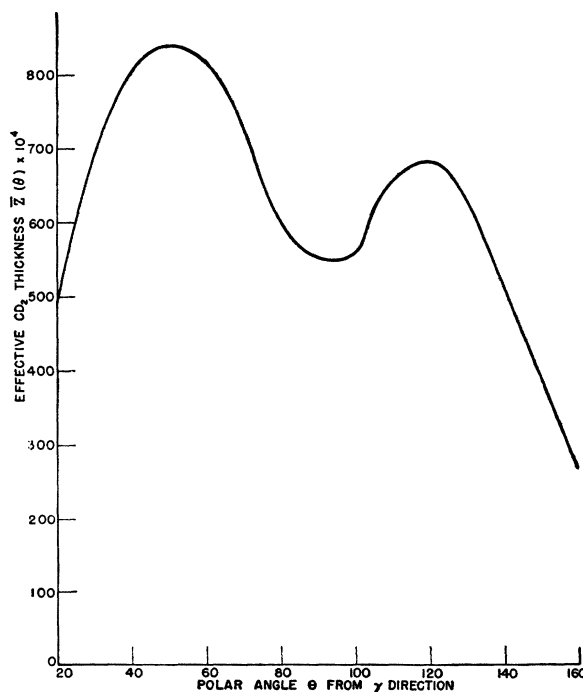


Fig. 5. Effective thickness, $\bar{Z}(\theta)$, of the CD₂ radiator (see text).

¹² Obtained by graphical integration of the dotted curves of Fig. 4b, reference 8.

TABLE III. The differential cross section at the mean energy of the lithium γ -rays.

Polar angle θ°	Number of tracks opposite CD ₂	Background	Differential cross section $\bar{\sigma}(\theta) \times 10^{29}$ cm ² /steradian
20-29	4	1	2.2±1.3
30-39	15	2	5.6±1.6
40-49	17	3	4.3±1.3
50-59	24	3	5.6±1.3
60-69	42	3	9.8±1.6
70-79	51	3	13.4±2.0
80-89	27	4	7.2±1.4
91-100	31	6	8.0±1.6
101-110	29	5	7.4±1.4
111-120	24	5	5.6±1.3
121-130	21	5	5.2±1.3
131-140	9	3	2.5±1.1
141-150	3	1	1.3±0.9
151-160	3	1	2.5±1.8

obtains for $\bar{Z}(\theta)$ the result shown in Fig. 5. The main features of the curve are readily understood. The decrease in the "effective thickness" of the radiator for θ near 0° and 180° occurs because at these angles only protons originating near the radiator surface will have sufficient projected range in the emulsion to be recorded. The depression near $\theta=90^\circ$ is chiefly the result of the loss of the tracks so nearly normal to the emulsion surface that complete penetration of the emulsion cannot give sufficient projected range. The forward peak is larger than the backward one because the forward protons have somewhat higher energy.

The final plates were exposed for about 20 hours with an average cyclotron beam current of 75 μ amp. Three lead-encased Geiger counters served to integrate the γ -ray intensity. The counters were checked from time to time with a radium source, and were calibrated absolutely 12 days after the run (see Sec. IV).

The use of dry emulsions made the subsequent searching and track measurement much less difficult and led to an observer efficiency, $\epsilon=0.91\pm 0.05$. The results obtained from a survey of two 1-inch by 3-inch NTB 200-micron plates are shown in Table III. Column 2 gives the number of tracks found in the emulsion region opposite the CD₂ radiator which satisfy the acceptance criteria given above and which fall within the range of polar angle shown in column 1. Column 3 gives the number of similar tracks found in the emulsion region opposite the graphite and CH₂, corrected for the difference in search areas. The fourth column gives the absolute differential cross section $\bar{\sigma}(\theta)$ calculated from Eq. (7) with the value for Γ given in Sec. IV.

For comparison with the theory, the experimental cross section is averaged over the 30° angular ranges centered on 60° , 90° , and 120° , and over the 25° ranges centered on $32\frac{1}{2}^\circ$ and $147\frac{1}{2}^\circ$. (The point at 90° is raised above the average cross section by 0.1×10^{-28} cm² to take account of the curvature in the experimental curve.) The laboratory system cross sections are then reduced to center-of-mass system cross sections by use

of the relation

$$\sigma_{CM}(\theta+4.0^\circ \sin\theta) = \sigma_{lab}(\theta)/[1+(8/57) \cos\theta].$$

Denoting the angle of disintegration in the center-of-mass system by ϕ , we plot the experimental values for $\sigma_{CM}(\phi)$ in Fig. 6. The solid curve also shown is that calculated by Marshall and Guth¹³ (their Fig. 4) normalized to give a total cross section $\bar{\sigma}_t = 7.6 \times 10^{-28}$ cm². This value for $\bar{\sigma}_t$ corresponds to a total cross section at 17.6 Mev of 7.0×10^{-28} cm², which is the value calculated from Eq. (6) of Bethe and Longmire¹⁴ with the new experimental triplet effective range,¹⁵ $r_0 = 1.74 \times 10^{-13}$ cm. It is to be noted that there is no adjustable parameter in either the experimental or the theoretical results.

The cross section averaged forward and back, $(\frac{1}{2})[\sigma_{CM}(\phi) + \sigma_{CM}(\pi - \phi)]$ is found to be well represented by Eq. (2), with θ replaced by ϕ and with

$$a = 0.02 \begin{matrix} +0.14 \\ -0.02 \end{matrix}$$

The laboratory differential cross section is integrated numerically by use of the data of Table III and yields for $\bar{\sigma}_t$ the value,

$$\bar{\sigma}_t = (7.8 \pm 1.5) \times 10^{-28} \text{ cm}^2. \quad (8)$$

From Eq. (6) and the intensity and cross-section ratios given after Eq. (7), we find for the total cross section at 17.6 Mev,

$$\sigma_{2t} = (7.2 \pm 1.5) \times 10^{-28} \text{ cm}^2. \quad (9)$$

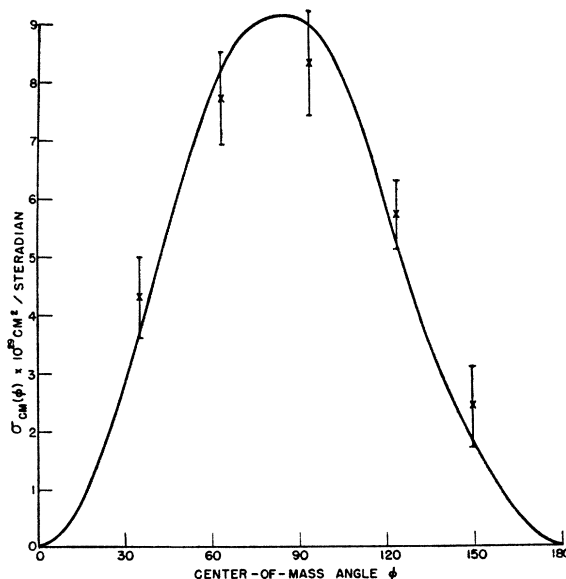


FIG. 6. Absolute differential cross section in the center-of-mass system at the mean energy of the lithium γ -rays. The crosses are the experimental values, and the solid curve is that calculated by Marshall and Guth.

¹³ J. F. Marshall and E. Guth, Phys. Rev. **78**, 738 (1950).

¹⁴ H. A. Bethe and C. Longmire, Phys. Rev. **77**, 647 (1950).

¹⁵ D. J. Hughes, Phys. Rev. **78**, 315 (1950). Hughes, Burgy, and Ringo, Phys. Rev. **77**, 291 (1950).

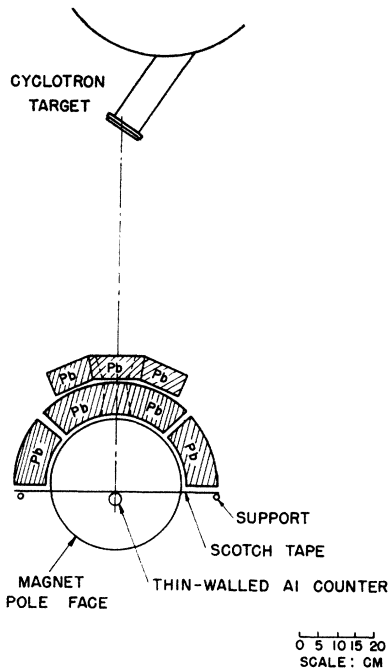


Fig. 7. Experimental arrangement for the absolute measurement of the intensity of the lithium gamma-radiation.

The essential limitation in the measurement is in the finite γ -ray source size, which means that the source-radiator distances x_1 and x_2 in Eq. (7) are known only to about 10 percent.

IV. ABSOLUTE MEASUREMENT OF THE γ -RAY INTENSITY

At the energies of the lithium γ -rays, the principal processes responsible for γ -ray absorption are pair production and the Compton effect. In either process nearly all of the secondary electrons are produced within a narrow cone whose axis is in the direction of the γ -ray. A thin lead foil placed directly before a sufficiently large counter exposed to the high energy γ -rays should therefore contribute an additional counting rate just equal to the number of absorption processes per second occurring in the foil. Since the total cross section for the γ -ray absorption in lead is known from the work of Walker,¹⁶ measurement of this additional counting rate gives the incident γ -ray intensity. Ninety percent of the absorption in lead is the result of pair production and, since only one of the pair electrons must pass through the counter to register the event, the situation is especially favorable with regard to loss of counts through scattering.

The experimental arrangement which was adopted¹⁷ is shown in Fig. 7. The γ -ray beam from the cyclotron target is collimated and enters a magnetic field of about

3000 gauss which sweeps out electrons originating in the collimator. A Victoreen aluminum Geiger counter of wall thickness 30 mg/cm² and sensitive area about 2 cm \times 5 cm is mounted vertically in the magnetic field with Scotch Tape. Thin lead foils of lateral dimensions 1 cm \times 2 cm are attached to the front of the counter, also with Scotch tape. Calling the counting rate of the Victoreen counter V , we may write

$$V = V_0 + (N_0 w / A) \bar{\sigma}_e g, \quad (10)$$

where V_0 is the counting rate with no foil, N_0 is Avogadro's number, w is the foil weight in grams, A is the atomic weight of lead, and g is the number of γ -rays per cm²-sec. at the foil.

$\bar{\sigma}_e$ is the average non-nuclear absorption cross section of lead for the lithium γ -rays and is calculated in the following way. Walker¹⁶ gives for the total cross section of lead at 17.6 Mev $\sigma = 20.56 \pm 0.12$ barns. If we subtract the (γ, n) cross section in lead, estimated¹⁸ to be 0.3 barn, we obtain a non-nuclear absorption cross section, $\sigma_e = 20.3 \pm 0.1$ barns. Using the theoretical ratio¹⁹ $\sigma_e(14.8) / \sigma_e(17.6) = 0.940$ and assuming the intensity ratio of the two lines given after Eq. (7), we get $\bar{\sigma}_e = \sigma_e(14.8) [I_1 / (I_1 + I_2) + \sigma_e(17.6) [I_2 / (I_1 + I_2)] = 19.6 \pm 0.1$ barns.

Equation (10) applies only for w so small that scattering and absorption of the secondary electrons and absorption of the primary gamma-radiation are negligible. These effects will contribute a negative term in Eq. (10) proportional to w^2 (for small w) and are negligible as long as the experimental curve of V against w is straight.

The quantity actually determined experimentally is not V , but

$$V/m_3 = (V_0/m_3) + (N_0 \bar{\sigma}_e / A) (g/m_3) w, \quad (11)$$

where m_3 denotes the counting rate of one of the lead-encased monitor counters (see Section III). V/m_3 is shown as a function of w in Fig. 8. The foil weight, $w = 1.5$ grams, where the curve begins to deviate from linearity, corresponds to a 4 percent absorption of the primary beam. The measured slope of the straight line portion is $(1.35 \pm 0.10) \times 10^{-2}$ (gram)⁻¹. With the value for $\bar{\sigma}_e$ given above, we obtain $g/m_3 = 0.238 \pm 0.019$.

(One measurement was made using an aluminum foil instead of lead. For equal values of $N_0 \bar{\sigma}_e g / A$, the two materials gave counting rates above background in the ratio of their cross sections, $\bar{\sigma}_e$ at the mean lithium energy, to within the statistical error of 5 percent in the counting rate ratio. McDaniel¹⁸ has compared lead, aluminum, and copper, with similar results. Since the relative absorption cross sections of the three elements

¹⁸ McDaniel, Walker, and Gorman (to be published.) Our estimate, which does not need to be accurate, is taken from their preliminary measurements. I wish to thank these authors for making their results available before publication.

¹⁹ P. V. C. Hough, Phys. Rev. **73**, 266 (1948). W. Heitler, *Quantum Theory of Radiation* (Oxford University Press, London, 1936).

¹⁶ R. L. Walker, Phys. Rev. **76**, 527 (1949).

¹⁷ A similar arrangement was used first by M. Camac (private communication). The general method was proposed by R. R. Wilson.

vary strongly with energy, these results serve to rule out any large proportion of degenerated γ -rays in the beam leaving the collimator. The aluminum-lead comparison shows, for example, that less than 8 percent of the γ -rays leaving the collimator have energies between 1 and 5 Mev; similar limits are obtained for other energy ranges.)

Now let M_3 represent a total number of monitor counts, and Γ the corresponding total number of lithium γ -rays emitted at the cyclotron target. Since the emission is known to be isotropic,²⁰ we have $g/m_3 = T(\Gamma/M_3)/4\pi R^2$, where R is the cyclotron target-Victoreen counter distance, and $T=0.96$ is the calculated transmission of the $\frac{1}{8}$ inch of aluminum and $\frac{1}{2}$ inch of water which intervene. For the exposure of the plates described in Section III, $M_3=3.61\times 10^6$ and, taking $R=1$ meter, we find $\Gamma=(1.12\pm 0.10)\times 10^{11}$. Through error, the monitor counters were moved before R was measured precisely, and it is necessary to increase the error to ± 0.2 . A completely independent earlier calibration of the monitor counters by Walker²¹ using the pair spectrometer leads to the value $\Gamma=(0.9\pm 0.2)\times 10^{11}$. We adopt $\Gamma=(1.01\pm 0.15)\times 10^{11}$ as the final value for the source strength used in Section III.

It seems likely that the above method for the absolute measurement of γ -ray intensity is capable of an accuracy of better than 5 percent.

V. COMPARISON WITH OTHER EXPERIMENTS AND WITH THE THEORY

Table IV gives the results of all the recent published measurements of the isotropic component, a , in the

TABLE IV. The isotropic component a in the differential cross section and the total cross section σ_t for the photo-disintegration of the deuteron.

γ -ray energy (Mev)	a (experiment)	a (theory)	$\sigma_t \times 10^{28}$ cm ² (experiment)	$\sigma_t \times 10^{28}$ cm ² (theory)
6.13	0.1 ^a	0.03 ^c	21.5 ± 1.2^d	21.2 ^e
	$0.02^{+0.04^b}_{-0.02}$			
17.6	$\sim 0.2^f$	0.01 ^c	8 ± 3^g	7.0 ^e
	$0.02^{+0.14^b}_{-0.02}$		8.5 ± 1.2^d	
			7.2 ± 1.5^h	

^a G. Goldhaber, Phys. Rev. **74**, 1725 (1948).

^b Present work.

^c H. A. Bethe, *Elementary Nuclear Theory* (John Wiley and Sons, New York, 1947).

^d Barnes, Stafford and Wilkinson, Nature **165**, 69 (1950).

^e H. A. Bethe and C. Longmire, Phys. Rev. **77**, 647 (1950). A triplet effective range, $r_0=1.74 \times 10^{-13}$ cm, is used.

^f E. G. Fuller, Phys. Rev. **79**, 303 (1950).

^g H. Waffler and S. Younis, Helv. Phys. Acta **22**, 414 (1949).

²⁰ Ageno, Amaldi, Bocciarelli, and Trobacchi, Ricerca Scient. **12**, 139 (1941).

²¹ R. L. Walker, private communication.

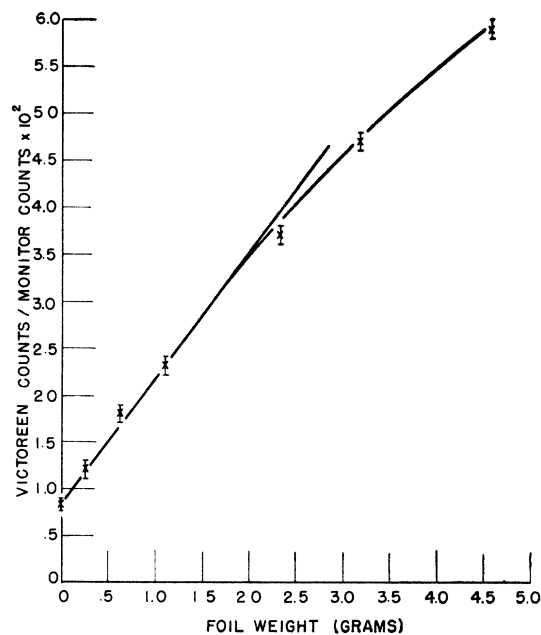


FIG. 8. Showing the counting rate of the Victoreen thin-walled aluminum Geiger counter, relative to the counting rate of a monitor counter, as a function of the weight of a lead foil attached to the front of the Victoreen counter.

differential cross section, and of the total cross section, σ_t , at the γ -ray energies of 6.13 and 17.6 Mev. (For an estimate of a at some intermediate energies, see reference 5.) The theoretical results quoted assume a free P -wave, and are calculated as described before Eq. (8).

Since most of these experiments were undertaken the high energy neutron-proton scattering experiments at Berkeley²² have shown that the P -state force is much smaller than the S -state force. Consequently, very precise measurements of the photo-disintegration cross section are required at 17.6 Mev to give independent evidence for the nature of the neutron-proton interaction. The present experiments are in good agreement with the simple theory of the process.

I wish to thank Professor Robert R. Wilson for suggesting this problem and for his continuing help and encouragement throughout the work. For assistance in the searching of plates and measurement of tracks I owe thanks to Mrs. M. R. Keck and especially to Mr. T. E. Palfrey, who gathered most of the high energy data. Mr. Bruce Dayton's help with the cyclotron is gratefully acknowledged. This work was begun while the author held the Eastman Kodak Company fellowship at Cornell University.

²² See, for example, R. S. Christian and E. W. Hart, Phys. Rev. **77**, 441 (1950).